by M. Ragulskis and R. Maskeliunas

MEASUREMENT OF TRANSVERSE VIBRATIONS OF PIEZOELECTRIC CERAMICS BY ATOMIC FORCE MICROSCOPY

Submicrometer amplitude vibrations play an important role in different physical and engineering systems. Ultrasonic motors are typical examples of application of such vibrations. The vibration energy of piezoelectric ceramics is transferred to longitudinal or rotational motion of the elements of these motors.[1–3]

Experimental measurement of transverse vibrations of piezoceramics excited by an oscillating charge is a complicated technical challenge first of all due to the fact that the amplitudes of these oscillations are small. The problem gets even harder when the frequency of excitation is far from the resonance frequencies of piezoelectric ceramics.[4] Pseudostatic (low frequency) excitation produces even smaller deformations of the piezoelectric ceramics. Nevertheless, the possibility of direct registration of transverse oscillations of electrically excited piezoceramics would be of great interest not only for the designers of ultrasonic motors[5] but also for many others in different applications of piezoelectric materials.[6,7]

Atomic force microscopy (AFM) is effectively applied for the measurement of nanoscale displacement, strain, and thermal deformation fields.[8–10] This paper is focused on the applicability of AFM for the measurement of dynamic displacements of electrically excited piezoelectric ceramic materials even far away from their resonance frequencies.

NUMERICAL MODEL

Let us assume that a flat nondeformable surface is parallel to plane $x-y$ and performs harmonic oscillations in the z-direction (Fig. 1). The amplitude of oscillations is A; angular frequency and phase—ω and φ. The AFM scanner is operating in the tapping mode; the maximum travel of the plane in the x-direction is L. Such raster-type back and forth scan produces a scanning path as shown in Fig. 1. It is assumed that the modulus of the scanner's travel velocity v in the x-direction is constant; distance between the raster lines is d; scanning direction is reversed instantaneously. The output of the measurement system is the instantaneous height of the scanned surface.

It is clear that the elevation of the scanned surface will be falsely represented by height. How would the scanned image of such a flat oscillating surface look like and how could it be interpretable? A simple numerical model is built in order to answer these questions.

Let us assume that the scanner starts the scanning process at time moment t_0. Then, the scanned instantaneous height at the right end of the first scanning line (Fig. 1) is $A\sin(\omega t_0 + \varphi)$. The time needed for the scanner to travel along the first scanning line is L/v. Thus, the scanned height at any x along the first scanning line (forward scan) is:

$$A\sin\left(\omega\left(t_0+\frac{x}{v}\right)+\varphi\right)=A\sin\left(\frac{\omega}{v}x+\delta_0\right) \tag{1}$$

where $\delta_0 = \omega t_0 + \varphi$. The time needed to return to the beginning of the second scanning line from the end of the first scanning line is also L/v. Then, the scanned height along the second scanning line is:

$$A\sin\left(\frac{\omega}{v}x+\frac{2L\omega}{v}+\delta_0\right) \tag{2}$$

In other words, the graph of the harmonic function in the second scan (Eq. 2) is shifted to the left by phase $2L\omega v^{-1}$ with respect to the first scan (Eq. 1). Keeping in mind that the functions are harmonic (with period $\frac{2\pi v}{\omega}$), the observed shift is $\arg(2L\omega v^{-1})$. Here, the function arg is defined as:

$$\arg(x)=x+k\frac{2\pi v}{\omega};\ k\in Z,\ -\frac{\pi v}{\omega}<\arg(x)\leqslant\frac{\pi v}{\omega} \tag{3}$$

Then, the angle of the observed shift is (Fig. 2):

$$\alpha=\arctan\left(\arg\left(2L\omega v^{-1}\right)/d\right) \tag{4}$$

It can be noted that due to the fact that the observed shift will always fit into one-period length interval around the reference peak (Fig. 2), the angle of the observed shift will always fall into the following interval:

$$-\arctan\left(\frac{\pi v}{d\omega}\right)<\alpha\leqslant\arctan\left(\frac{\pi v}{d\omega}\right) \tag{5}$$

If the scanning direction would be reversed, the total shift would be $-2L\omega v^{-1}$ and the angle of the observed shift would be:

$$\alpha=\arctan\left(\arg\left(-2L\omega v^{-1}\right)/d\right) \tag{6}$$

Numerical simulations of a scanning process over a flat oscillating plate reveal the effect of the formation of grating caused by false representation of the surface elevation by height (Fig. 3a, b) at $L = 3$ μm, $v = 3$ μm/s, $A = 0.2$ μm, and $d = 0.03$ μm, with the direction of scanning from right to left.

TECHNIQUE FOR IDENTIFICATION OF TRANSVERSE VIBRATIONS

The formation of an observable grating caused by oscillation of a scanned surface can be effectively exploited for the identification of parameters of that oscillation. The identification

M. Ragulskis is a professor in the Department of Mathematical Research in Systems at Kaunas University of Technology, Kaunas, Lithuania. R. Maskeliunas (SEM Member) is an associate professor in the Department of Printing Machines at Vilnius Gediminas Technical University, Vilnius, Lithuania.

doi: 10.1111/j.1747-1567.2006.00020.x

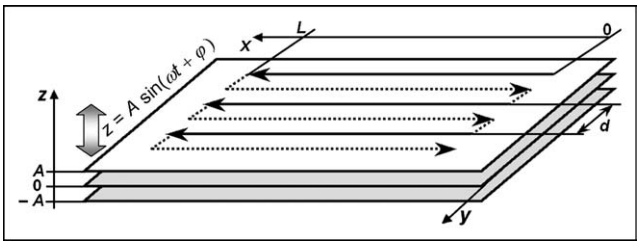

Fig. 1: Scan over an oscillating plate—a schematic diagram

of the angular frequency of oscillation is straightforward and comprises two basic steps:

(1) The distance between the centers of grating lines λ must be measured along the scan direction.

(2) Then, the angular frequency of oscillations can be determined from the following equation:

$$\omega = \frac{v}{\lambda} \tag{7}$$

The amplitude of oscillation can be determined by analyzing the scanned surface in a three-dimensional (3D) projection, though it is a much more complex problem involving the physical interaction between the tip and the surface. The angle of the grating lines is an effect of secondary importance, though it could be used for the identification of the scan direction.

EXPERIMENTAL MEASUREMENT OF TRANSVERSE VIBRATIONS OF PIEZOELECTRIC CERAMICS

The experimental setup comprises an AFM, piezoelectric ceramics (5 × 10 × 3 mm) placed on the measurement table, and a power amplifier producing oscillating charge (Fig. 4). Two thin copper wires (0.05-mm diameter each) are welded to the side electrodes of the ceramics and connected to the power amplifier (Fig. 5). The scanning area is set to 3.2 × 3.2 μm (the maximum travel of the scanner L = 3.2 μm). The sweep frequency is 1 Hz—the scanner sweeps over the scanning area forward and backward in 1 s; scanning speed v = 6.4 μm/s. The produced digital image of the scanned area consists of 512 × 512 pixels (512 scan lines in forth or in back direction);

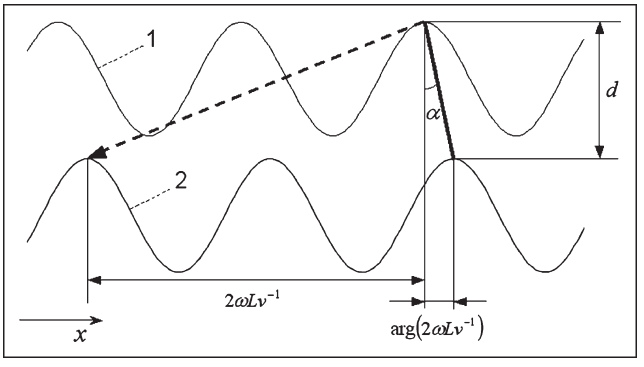

Fig. 2: The observed shift between scanning lines: 1, the first line; 2, the second line of the forward scan

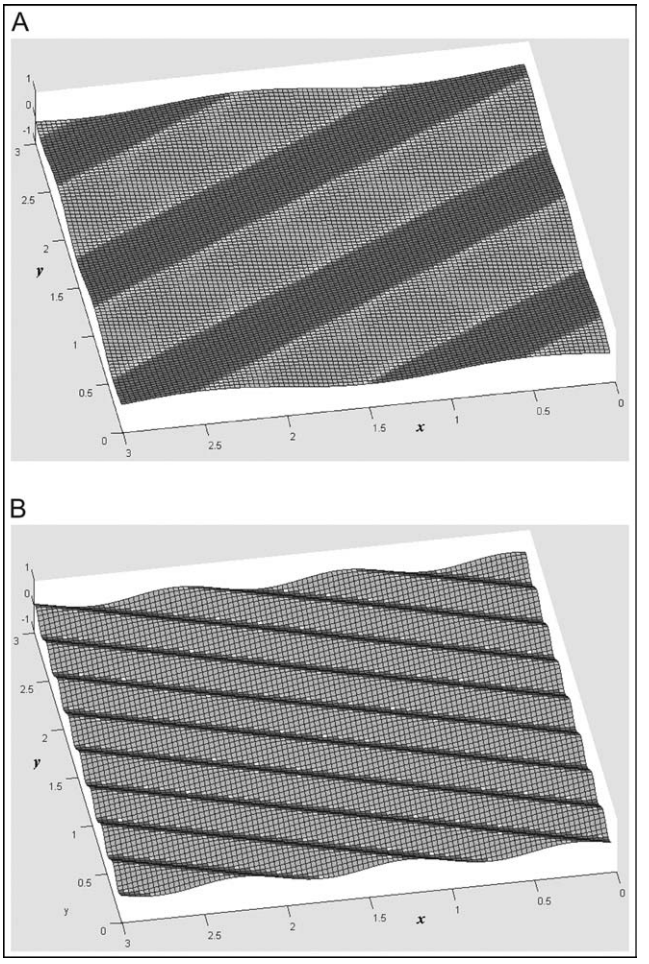

Fig. 3: Numerical simulations of forward scan at L = 3 μm, v = 3 μm/s, A = 0.2 μm, d = 0.03 μm; (a) ω = 9.5 Hz; (b) ω = 18.6 Hz

d = 0.00625 μm. Time required to perform full surface scan is 512 s.

The experimental image of the piezoelectric ceramics excited by an 8-Hz frequency oscillating charge is shown in Fig. 6.

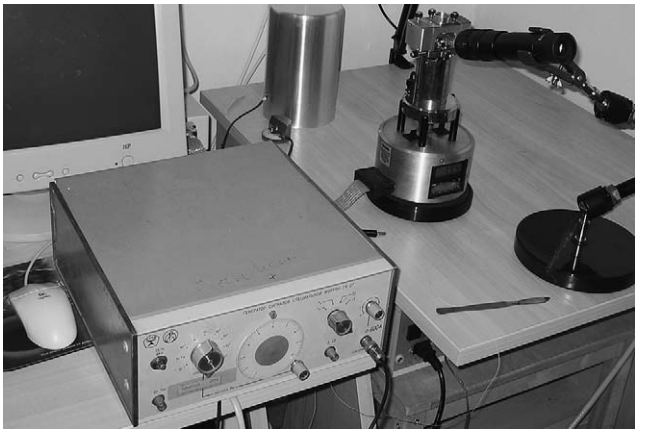

Fig. 4: View of the experimental setup

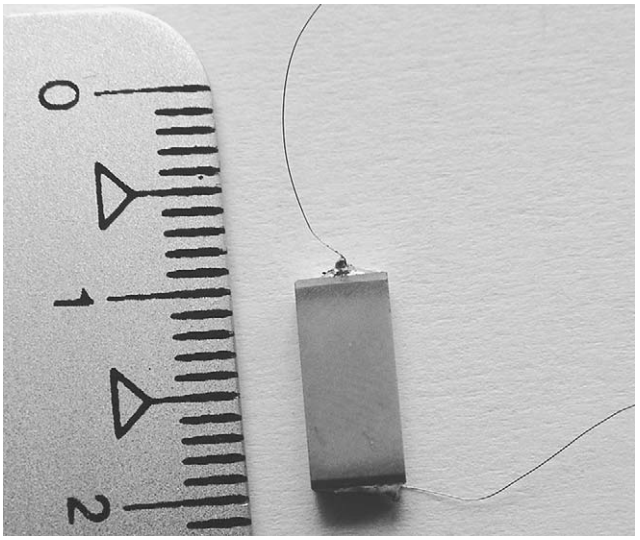

Fig. 5: Piezoelectric ceramics with welded electrode wires

The forth scan in 3D projection is shown in Fig. 6a and back scan in 2D projection in Fig. 6b. It can be noted that the oblique trenched grating is an effect caused by the transverse oscillation of the surface of the sample, which in its turn is a direct result of the excitation of the piezoceramics. It can be noted that the number of grating lines per scan line is about four, which produces $\lambda = 0.8\ \mu$m. This is a perfect result validating Eq. 7.

The time needed to perform the full surface scan is more than sufficient for manual adjustments of the excitation frequency of the piezoceramics. Though Fig. 6 clearly illustrates the formation of gratings due to the oscillatory elevation of the surface, it would be of a certain interest to observe the behavior of the pattern of fringes when the excitation frequency is changed during the scanning process. The experimental setup for such a measurement is identical to the one used for the generation of digital AFM images shown in Fig. 6. The only exception is that the frequency control handle of the signal generator (Fig. 4) is manually turned clockwise and counterclockwise several times during the scanning process, thus increasing or decreasing the excitation frequency of the piezoceramics. Such measurement allows one not only to observe the "real-time" response of piezoceramics to the changing excitation but also to detect possible transient processes taking place after the frequency is changed. Moreover, produced analytical relationships may help to reconstruct actual excitation frequencies at different time intervals.

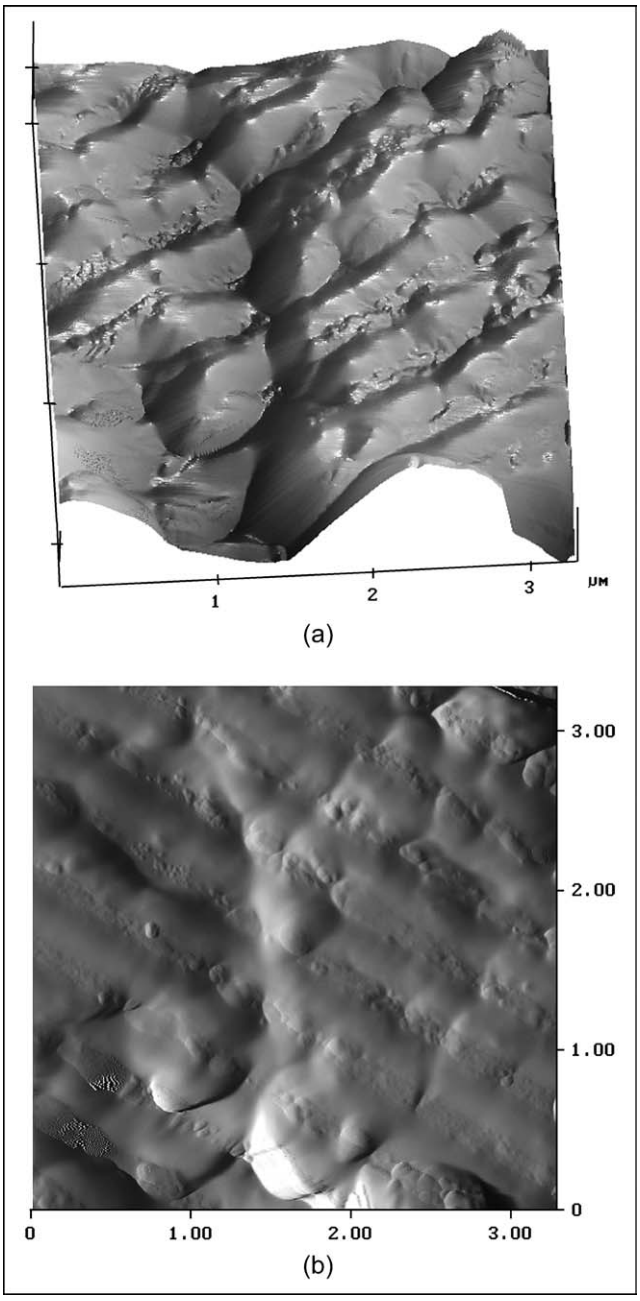

Fig. 6: Digital image of the scanned surface: (a) 3D projection; (b) 2D projection

Figure 7 shows the experimental image of excited piezoelectric ceramics at different frequencies of excitation. The AFM image is constructed for the forward scan. The scanner travels from right to left; the scan lines are ordered from top to bottom in time scale (Fig. 1). The frequency of excitation was changed six times during the scanning process. This is illustrated in Fig. 7b; every segment Δ_i represents a time interval when the excitation frequency was kept constant.

The image of the scanned surface clearly illustrates the fact that the observed grating is a result of transverse oscillation of the piezoceramics. It can be noted that in some time segments (particularly in Δ_5 and Δ_6), the fringes are hardly interpretable. In order to make the pattern of fringes more clear, arrays of white stripes are placed on the center of the fringes (Fig. 7b). Every individual stripe is placed using computer mouse "click-and-drag" technique. The digital AFM image is filtered before drawing the stripes what makes the placement of lines along the center of fringes easier. Sophisticated digital image processing procedures used in automatic fringe counting techniques[11] can be exploited to generate the composite patterns of fringes in case higher reconstruction uncertainties are required. The results of the analysis of Fig. 7b are shown in Table 1.

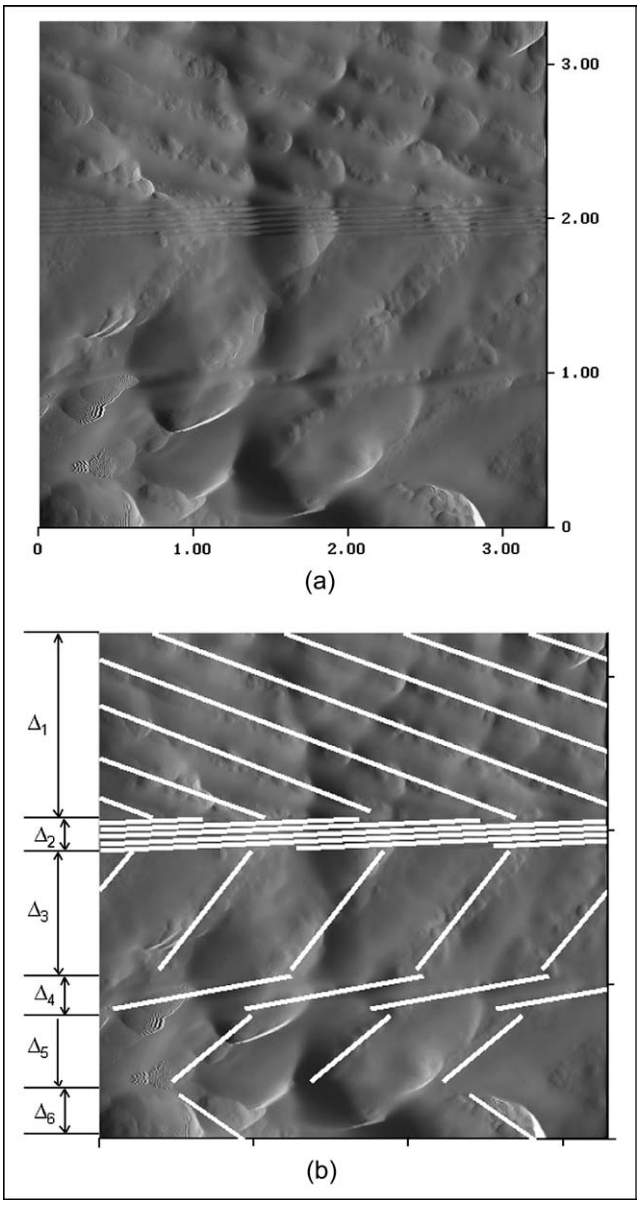

Fig. 7: Digital image of the scanned surface at varying frequencies of excitation: (a) experimental image; (b) marked white grating lines on top of the image

It can be noted that the distance between fringes must be measured in the direction of the scanning line. Therefore, the observed density of fringes in the zone Δ_2 does not contribute to the smallness of parameter λ (Table 1). The angle of grating is determined by Eq. 4 and is rather sensitive to the variation of ω.

Also, one must have in mind that the presented technique is applied for analysis of experimental AFM images. So, the reconstructed frequency is the physical frequency of transverse oscillations of piezoelectric ceramics, not its excitation frequency. Nevertheless, the experimental results demonstrate that the duration of transient processes (after the excitation frequency is changed) is very small and only the steady-state reaction of piezoceramics is observed. Therefore, the excitation and the reaction frequencies can be considered the same even in the presence of complex material properties (like dynamic viscoelasticity).[12]

Table 1—Determination of the frequency of excitation

DESCRIPTION OF THE ZONE	SCANNING TIME IN EACH ZONE (s)	DISTANCE BETWEEN FRINGES λ (μm)	EXCITATION FREQUENCY ω (Hz)
Δ_1	187	0.754	8.48
Δ_2	33	0.937	6.83
Δ_3	125	0.833	7.69
Δ_4	42	0.807	7.94
Δ_5	75	0.859	7.45
Δ_6	50	1.847	3.46

The observable grating caused by the periodic elevation of the measured surface can be used for identification of the amplitude of vibrations. Periodic elevations are modulated on top of the static surface structure of the sample. Nondimensional amplitude of vibrations can be directly determined from 3D projections of the digital images. Calibration of the interpretable height then results into accurate determination of the nanoscale amplitudes.

Finally, it can be noted that the measured oscillations of the piezoelectric ceramics are far away from its resonance frequencies. The range of observable frequencies is restricted by the physical limitations of the presented technique. The lower range can be defined from the requirement that the sample surface performs at least one period of oscillation during the time the scanner travels along one scanning line. The upper range can be determined from AFM tapping frequency. At least 10 discrete measurement points should fit into one period of oscillation in order to produce an interpretable digital picture of the grating. In our experiment, these considerations result into the condition $0.0625 \leqslant \lambda \leqslant 3.2$ μm, which in turn determines the interpretable range of frequencies $2 \leqslant \omega \leqslant 102.4$ Hz.

CONCLUDING REMARKS

A technique for AFM measurement of transverse vibrations of piezoceramics is presented in this paper. Though the interpretable range of frequencies is rather limited, such measurements can be of a high value for testing properties of piezoelectric materials.

References

1. Pons, J.L., Rodríguez, H., Seco, F., Ceres, R., and Calderón, L., "Modelling of Piezoelectric Transducers Applied to Piezoelectric Motors: A Comparative Study and New Perspective," *Sensors and Actuators A: Physical* **110**(1/3):336–343 (2004).

2. Roh, Y., and Kwon, J., "Development of a New Standing Wave Type Ultrasonic Linear Motor," *Sensors and Actuators A: Physical* **112**(2/3):196–202 (2004).

3. Vasiljev, P., Borodinas, S., Yoon, S.J., Mažeika, D., and Kulvietis, G., "The Actuator for Micro Moving of a Body in a Plane," *Materials Chemistry and Physics* **91**(1):237–242 (2005).

4. Santana-Gil, A., Pelaiz-Barranco, A., and Rodriguez-Lopez, L., "Low-cost and Easy Experiment to Study the Electromechanical Resonance of Piezoelectric Ceramics," *Review of Scientific Instruments* **76**(1): Art. No. 013908:1–3 (2005).

5. Muneishi, T., and Tomikawa, Y., "Ultrasonic Linear Motor with Two Independent Vibrations," *Japanese Journal of Applied Physics* **43**(9B):6728–6732 (2004).

6. Eremkin, V.V., Smotrakov, V.G., Aleshin, V.A., and Tsikhotskii, E.S., "Microstructure of Porous Piezoceramics for Medical Diagnostics," *Inorganic Materials* **40**(7):775–779 (2004).

7. Li, E.Z., Chu, X.C., Gui, Z.L., and Li, L.T., "Vibration Characteristics of a Piezoelectric Sensor for Distance Measurement," *Rare Metal Materials and Engineering* **32**(1):605–608 (2003).

8. Liu, C.M., and Chen, L.W., "Digital Atomic Force Microscope Moire Method," *Ultramicroscopy* **101**(2/4):173–181 (2004).

9. Xie, H.M., Asundi, A., Boay, C.G., Lu, Y.G., Yu, J., Zhong, Z.W., and Ngoi, B.K.A., "High Resolution AFM Scanning Moire Method and Its Application to the Micro-deformation in the BGA Electronic Package," *Microelectronics Reliability* **42**(8):1219–1227 (2002).

10. Xie, H.M., Boay, C.G., Liu, T., Lu, Y.G., Yu, J., and Asundi, A., "Phase-shifting Moiré Method with an Atomic Force Microscope," *Applied Optics* **40**(34):6193–6198 (2001).

11. Kobayashi, A.S. (Editor), *Handbook on Experimental Mechanics*, 2nd Edition, SEM, Bethel, CT (1993).

12. Ragulskis, M., and Ragulskis, L., "On Interpretation of Fringe Patterns Produced by Time Average Photoelasticity," *Experimental Techniques* **29**(3):48–51 (2005). ■